Sensor and Actuator Selection for Large Space Structure Control

M. L. DeLorenzo*
Air Command and Staff College, Maxwell Air Force Base, Alabama

This paper presents an algorithm that aids the controls engineer in specifying a sensor and actuator configuration for regulation of large-scale, linear, stochastic systems such as a large space structure model. The algorithm uses a linear quadratic Gaussian controller, an efficient weight-selection technique based on successive approximation, and a measure of sensor and actuator effectiveness to specify a final sensor and actuator configuration. This configuration enables the closed-loop system to meet output specifications with minimal input power. The algorithm involves no complex gradient calculations and is numerically tractable for large linear models, as demonstrated by the solar optical telescope example in this paper. Additionally, the algorithm provides the controls engineer with information on the important design issues of actuator sizing, reliability, redundancy, and optimal number.

I. Introduction

THE advent of the Space Shuttle makes the large space structure (LSS) an imminent reality. These future space structures will be measured in kilometers and, of necessity, will be lightweight and highly flexible (light damping). Standard LSS missions will include power generation, surveillance, astronomy, and communications. These missions will require stringent pointing accuracy, shape control, and vibration suppression. To satisfy these demanding mission requirements, the LSS will almost certainly require an active, regulator-type controller with multiple sensors and actuators located throughout the structure.[1-6] Furthermore, given the size of an LSS, there will be a large set of admissible sensor and actuator locations. The controls engineer then faces the problem of selecting a limited number of sensor and actuator locations to "best achieve" the LSS mission. The term "best achieve" in this paper means achieving the LSS output specifications with minimal actuator power.

The solution to this sensor and actuator selection (SAS) problem needs at least the following ingredients: 1) A specific closed-loop control law structure; 2) a technique for systematically adjusting (tuning) control law parameters to achieve output specifications with minimal power; and 3) a technique to evaluate the effectiveness of possible sensor and actuator configurations in achieving output specifications with minimal power.

This paper incorporates the preceding ingredients into an algorithm that solves the SAS problem for an LSS modeled as a linear stochastic system. Some necessary background information on linear stochastic systems and linear quadratic Gaussian (LQG) control theory are presented in Sec. II along with a formal statement of the SAS problem. Section III contains two important selection theorems, four pertinent facts, and the general flow of the SAS algorithm. Results from the SAS algorithm applied to the controller design for a large space telescope are presented in Sec. IV, and Sec. V contains concluding remarks.

Received May 27, 1988; revision received Sept. 17, 1988.

*Major, U.S. Air Force; currently at Arnold Engineering Development Center, Arnold Air Force Base, TN.

II. Background

The SAS algorithm presented in this paper addresses the control of an LSS described by the following linear stochastic model:

$$\dot{x}(t) = Ax(t) + Bu(t) + Dw(t), \quad x \in \boldsymbol{R}^n, \; u \in \boldsymbol{R}^m, \; w \in \boldsymbol{R}^p \tag{1a}$$

$$x(t_o) = x_o \tag{1b}$$

$$D \equiv \begin{bmatrix} B & D_o \end{bmatrix}, \quad w(t) \equiv \begin{bmatrix} w_a^T(t) & w_o^T(t) \end{bmatrix}^T \tag{1c}$$

$$y(t) = Cx(t), \quad y \in \boldsymbol{R}^k \text{ (system outputs)} \tag{1d}$$

$$z(t) = Mx(t) + v(t), \quad z \in \boldsymbol{R}^l \text{ (system measurements)} \tag{1e}$$

with noise characteristics

$$E\begin{bmatrix} x_o \\ w(t) \\ v(t) \end{bmatrix} \begin{bmatrix} x_o^T, w^T(\tau), v^T(\tau) \end{bmatrix} = \begin{bmatrix} X_o & 0 & 0 \\ 0 & W\delta(t-\tau) & 0 \\ 0 & 0 & V\delta(t-\tau) \end{bmatrix} \tag{2}$$

$$Ex_o \equiv 0, \quad Ew(t) \equiv 0, \quad Ev(t) \equiv 0, \quad W > 0, \quad v > 0$$

The notation $\boldsymbol{R}^i$ implies a real vector space of dimension i. The expectation operator is denoted by E. The superscript T represents matrix transposition. The Dirac delta function is denoted by δ, and $W > 0$ implies W is a positive definite matrix. The n-dimensional vector $x(t)$ represents the state of the system, while the m-dimensional vector $u(t)$ contains actuator signals. The regulated system outputs are defined by the k-dimensional vector $y(t)$, and the l-dimensional vector $z(t)$ represents the system measurements (sensor information). The white-noise vector process $w(t)$ represents unmodeled system behavior $D_o w_o(t)$ and unmodeled actuator behavior $Bw_a(t)$. Unmodeled sensor behavior is accounted for by the white-noise vector process $v(t)$. The matrices A, B, C, D, M, W, and V are time-invariant and appropriately dimensioned. The matrix B has no zero columns, and the matrices C and M have no zero rows. Furthermore, the matrices A, B, C, D, and M satisfy the following stabilizability and detectability conditions:

$$\text{stabilizable: } (A,B),\ (A,D) \tag{3a}$$

$$\text{detectable: } (A,C),\ (A,M) \tag{3b}$$

For simplicity, the model described by Eqs. (1-3) will be identified by $S(n,k,m,l)$. The arguments n, k, m, and l represent the number of system states, outputs, actuators, and sensors, respectively.

$S(n,k,m,l)$ specifications usually take the form

$$\lim_{t\to\infty} Ey_i^2(t) \equiv E_\infty y_i^2 \le \sigma_i^2, \qquad i = 1,2,\ldots,k \tag{4}$$

$$\lim_{t\to\infty} Eu_i^2(t) \equiv E_\infty u_i^2 \le \mu_i^2, \qquad i = 1,2,\ldots,m \tag{5}$$

where y_i represents the ith output for the system, and u_i represents the ith input. The quantities σ_i^2, μ_i^2 are mean square or variance constraints on the ith output and input. These specifications are ideally suited for the LSS case where y_i could represent a line-of-sight pointing error, a deflection from a desired shape, etc., and u_i could be the output from a thruster, torque actuator, etc.

The ingredients of the SAS solution stated in Sec. I require the choice of a specific closed-loop control law that is readily adjusted to meet the output specifications with minimal power. LQG control theory provides such a law. This theory originated in the 1960's with the foundational work of Kalman, Bucy, and others. Since that time, many papers and texts have been written, further clarifying and expanding the theory. References 7-9 are a few examples. The following paragraphs present the fundamental results of the theory.

For a system $S(n,k,m,l)$, LQG theory guarantees a stable, steady-state, closed-loop control system minimizing

$$V = E_\infty(y^TQy + u^TRu) \tag{6a}$$

or

$$V = \sum_{i=1}^{k} E_\infty y_i^2 q_i + \sum_{i=1}^{m} E_\infty u_i^2 r_i \tag{6b}$$

where q_i and r_i are the ith diagonal entries of the arbitrary, diagonal, and positive definite weighting matrices Q and R. The defining equations for this steady-state controller are

$$u(t) = -R^{-1}B^TK\hat{x}(t) \equiv G\hat{x}(t) \tag{7a}$$

$$\dot{\hat{x}}(t) = A_c\hat{x}(t) + Fz(t), \qquad F \equiv PM^TV^{-1}$$

$$A_c \equiv A + BG - FM, \qquad \hat{x}(t_o) = x_o \tag{7b}$$

Steady-state control Riccati equation:

$$KA + A^TK - KBR^{-1}B^TK + C^TQC = 0 \tag{7c}$$

Steady-state filter Riccati equation:

$$PA^T + AP - PM^TV^{-1}MP + DWD^T = 0 \tag{7d}$$

Substituting this controller into $S(n,k,m,l)$, the following closed-loop system $S(2n,\ k+m,\ m+l,\ 0)$ results:

$$\dot{\bar{x}} = \bar{A}\bar{x} + \bar{B}\bar{w}, \qquad \bar{x} \equiv (x^T\hat{x}^T)^T, \qquad \bar{w} \equiv (w^Tv^T)^T$$

$$\bar{y} = \bar{C}\bar{x}, \qquad \bar{V} = \bar{y}^T\bar{Q}\bar{y}, \qquad \bar{y} \equiv (y^Tu^T)^T \tag{8a}$$

$$\bar{A} \equiv \begin{bmatrix} A & BG \\ FM & A_c \end{bmatrix}, \qquad \bar{B} \equiv \begin{bmatrix} D & 0 \\ 0 & F \end{bmatrix}$$

$$\bar{C} \equiv \begin{bmatrix} C & 0 \\ 0 & G \end{bmatrix}, \qquad \bar{Q} \equiv \begin{bmatrix} Q & 0 \\ 0 & R \end{bmatrix} \tag{8b}$$

Given the noise characteristics of $S(n,k,m,l)$, the steady-state variance matrix for $S(2n,\ k+m,\ m+l,\ 0)$ is known to be

$$E_\infty\left\{(\bar{x}-0)(\bar{x}-0)^T\right\} = E_\infty\left\{\bar{x}\bar{x}^T\right\} = \begin{bmatrix} \hat{X}+P & \hat{X} \\ \hat{X} & \hat{X} \end{bmatrix} \tag{9}$$

$$\hat{X} \equiv \lim_{t\to\infty}\hat{X}(t) \equiv E_\infty\left\{(\hat{x}-0)(\hat{x}-0)^T\right\} = E_\infty\left\{\hat{x}\hat{x}^T\right\} \tag{10}$$

where $\hat{X}$ is the solution of the steady-state Lyapunov equation

$$\hat{X}(A+BG)^T + (A+BG)\hat{X} + PM^TV^{-1}MP = 0 \tag{11}$$

Also, coupling the definition of $\bar{x}$ in Eq. (8a) with Eq. (9) gives

$$X \equiv \lim_{t\to\infty}X(t) \equiv E_\infty\left\{xx^T\right\} = \hat{X} + P \tag{12}$$

The following facts, documented in Refs. 10-14, show that the LQG control structure is extremely powerful in attacking the SAS problem:

F1) Analytical expressions for $E_\infty y_i^2$ and $E_\infty u_i^2$ exist and require no additional major calculations beyond those of the controller:

$$E_\infty y_i^2 = \left[C(P+\hat{X})C^T\right]_{ii}, \qquad i = 1,\ldots,k \tag{13}$$

and ii implies the ith diagonal element of the matrix

$$E_\infty u_i^2 = \left[G\hat{X}G^T\right]_{ii}, \qquad i = 1,\ldots,m \tag{14}$$

F2) A successive aproximation algorithm (LQGWTS) developed in Refs. 10, 13, and 14 can be used to adjust the elements of Q and R so that the LQG controller achieves the output specifications $E_\infty y_i^2 = \sigma_i^2$, $i = 1,\ldots,k$ with minimal power. That is,

$$\sum_{i=1}^{m} E_\infty u_i^2 = \min$$

LQGWTS involves no gradient calculations or complex calculation beyond the LQG controller and is numerically tractable for large systems as shown in Refs. 10, 13, and 14.

F3) A measure developed in Refs. 10 and 11 identifies the effectiveness of each sensor and actuator in the present LQG controller configuration. The mathematical expressions for these effectiveness values are

$$V_i^{\text{sen}} = m_i^TPLPm_iV_{ii}^{-1} \tag{15}$$

where m_i is the ith column of M^T, and

$$V_i^{\text{act}} = \left[G\hat{X}G^TR\right]_{ii} - \left[B^T(K+L)BW^a\right]_{ii} \tag{16}$$

where W^a is the partition of W corresponding to actuator noise sources $[w_a(t)]$, and L satisfies the following:

$$L(A - PM^TV^{-1}M) + (A - PM^TV^{-1}M)^TL + G^TRG = 0$$

Facts 2 and 3 represent recent contributions to LQG theory. Their derivations are in Ref. 10 but are omitted here for the sake of brevity. However, Appendix A presents a brief summary of the weight-selection work, and Appendix B provides a short discussion of the effectiveness values.

With the preceding background, the SAS problem addressed in this paper can be mathematically stated.

SAS Problem Statement

Given: A system $S(n,k,m,l)$ that has only $\bar{m}$ out of m actuators and $\bar{l}$ out of l sensors available to design a steady-state LQG regulator, which must achieve a set of output variances σ^2.

Required: Specify the closed-loop system that satisfies the following:

$$\min \sum_{i=1}^{\bar{m}} E_\infty u_i^2 \text{ subject to } E_\infty y_i^2 = \sigma_i^2, \qquad \forall i = 1,\ldots,k \quad (17)$$

III. SAS Algorithm

Before presenting the algorithm, two selection theorems and some pertinent facts should be stated.

Theorem 1: (Deletion of noisy actuators). For a system $S(n,k,m,l)$ regulated by the LQG controller defined in Eqs. (7), the deletion of an actuator is not sufficient for $V(m-1) > V(m)$, where

$V(m)$ = the value of Eqs. (6) for a system $S(n,k,m,l)$ under LQG regulation

$V(m-1)$ = the value of Eqs. (6) for a system $S(n,k,m-1,l)$ under LQG regulation

The proof of Theorem 1 is given in Ref. 10. More specifically, Theorem 1 says it is possible for an LQG controller to do better (i.e., maintain output specifications at a lower input power) when a noisy actuator is deleted. This means that the desired number of actuators in a control system might be less than the allowable number (i.e., $<\bar{m}$).

Theorem 2: (Deletion of noisy sensors). For a system $S(n,k,m,l)$ under the regulation of the LQG controller defined in Eqs. (7), deletion of a sensor cannot reduce the V of Eqs. (6).

Theorem 2 clearly says that noisy sensors never degrade the performance of an LQG controller. The proof of this theorem is contained in Refs. 10, 12, and 15. However, intuitively, it makes sense because the LQG controller uses a Kalman filter, and if a sensor is too noisy the Kalman filter essentially ignores the information from that sensor. Therefore, Theorem 2 indicates that the number of sensors in the controller design should be $\bar{l}$ (i.e., the allowable number).

The following facts are important to the algorithm:

F4) Data in Refs. 10 and 16 show relative V_i^{act} and V_i^{sen} rankings can change as functions of Q and R.

F5) Deleting sensors and actuators changes the Q and R needed to achieve output specifications at minimal power.

F6) The results from Refs. 10, 11, 15, and 17 show that the SAS problem is highly coupled and simultaneous SAS works better than sequential selection.

F7) V_i^{sen} and V_i^{act} do not predict the loss of measurability or controllability.

With these theorems and facts stated, the general flow of the SAS algorithm can be outlined.

SAS Algorithm (General Flow)

1) Given the system $S(n,k,m,l)$, specify the number of sensors $\bar{l}$ ($\bar{l}<l$) and actuators $\bar{m}$ ($\bar{m}<m$) that can be used in the controller design.

2) Run the subroutine LQGWTS for the full system $S(n,k,m,l)$. [LQGWTS selects the weighting matrices Q and R so that the LQG controller enables the closed-loop system to satisfy Eq. (17).]

3) With the resulting closed-loop system, calculate V^{sen} and V^{act} for each sensor and actuator using Eqs. (15) and (16).

4) Rank the actuators and sensors according to the algebraic value of V^{sen} and V^{act}.

5) Modify the current system to eliminate the lowest ranking sensor and actuator and all others of "nearly" the same ranking, if measurability and/or controllability of the system are not disturbed.

6) If the appropriate number of actuators and sensors are deleted (i.e., $m-\bar{m}$ and $l-\bar{l}$), stop. However, in light of Theorem 1, fewer actuators than $\bar{m}$ may be better, and actuator deletion should continue until

$$(1/m^*)\sum_{i=1}^{m^*} E_\infty u_i^2 \quad (18)$$

is no longer decreasing. [*Note*: m^* is the number of actuators currently in the design ($m^*<\bar{m}$), and Eq. (18) is the average power per actuator.]

7) Run LQGWTS on the reduced system and return to step 3.

Facts 4 and 5 dictate the order of steps 2, 3, and 4 in the preceding general flow. More specifically, since the ranking of effectiveness values can vary as a function of Q and R, the effectiveness values should be based on the Q and R that produce a closed-loop system satisfying Eq. (17).

Step 5 of the general flow results form facts 6 and 7. Caution should be exercised in deleting sensors and actuators with "nearly" the same effectiveness values since facts 4 and 5 indicate that any perturbation in the sensor and actuator configuration can alter relative effectiveness rankings of the sensors and actuators. Also, the requirement for checking measurability and controllability is severe. However, as a result of the work by Hughes and Skelton,[18] the controllability and measurability of systems in modal form (i.e., the form of the telescope model in Appendix C) can be done by inspection for systems of any dimension.

Theorems 1 and 2 provide the rationale for step 6. If $\bar{l}$ sensors are allowed, then according to Theorem 2, $\bar{l}$ sensors should be used. Theorem 1 invalidates this philosophy for actuators.

IV. Space Telescope Example

This section presents the results of the SAS algorithm when applied to the model of a solar optical telescope. Before discussing the results, a brief model description is presented.

The solar optical telescope model was developed in 1980 by the Charles Stark Draper Laboratory (CSDL) primarily to provide a minimum complexity structure to evaluate LSS control design techniques. The outputs for the model are the telescope line-of-sight (LOS) angles about the x and y axes (see Fig. 1) and the focal length (defocus) of the lenses located at the top and bottom of the telescope.

The 12 nodes shown in Fig. 1 represent the spatial locations for 45 admissible sensors and 21 admissible actuators. Tables 1–3 provide specific type, location, direction, and label information for the admissible sensors and actuators and also a listing of the output specifications σ.

CSDL used the program NASTRAN to develop data for the first 44 mode shapes of the telescope and to provide location information for the two sinusoidal disturbances S_1 and S_2 shown in Fig. 1. The final design model chosen for this example was a 10-mode, 20-state, linear stochastic model coupled with a 2-mode, 4-state, linear stochastic model of the distur-

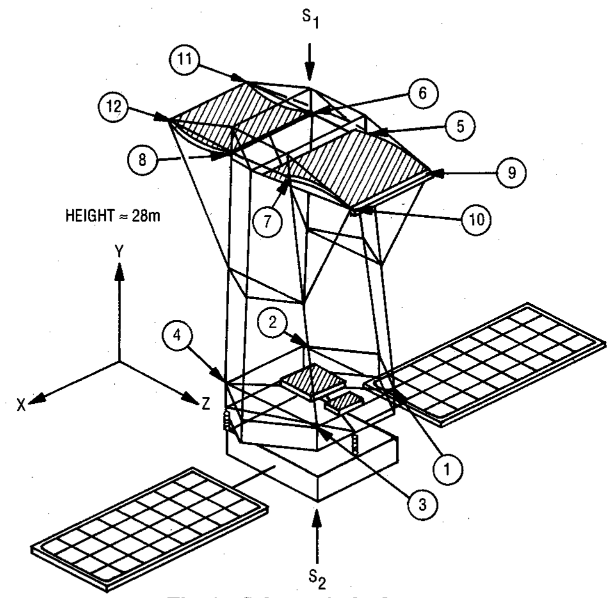

Fig. 1 Solar optical telescope.

Table 1 Telescope sensor description

Sensor no.	Type	Nodal location	Direction	Label
1	Line-of-sight angle	—	X	LOS_x
2	Line-of-sight angle	—	Y	LOS_y
3	Defocus	—	—	Defocus
4	Linear displacement	1	Y	Y1
5	Linear displacement	1	Z	Z1
6	Linear displacement	2	Z	Z2
7	Linear displacement	3	X	X3
8	Linear displacement	3	Y	Y3
9	Linear displacement	3	Z	Z3
10	Linear displacement	4	Z	Z4
11	Linear displacement	5	X	X5
12	Linear displacement	5	Y	Y5
13	Linear displacement	5	Z	Z5
14	Linear displacement	6	Z	Z6
15	Linear displacement	7	Y	Y7
16	Linear displacement	7	Z	Z7
17	Linear displacement	8	Z	Z8
18	Linear displacement	9	Z	Z9
19	Linear displacement	10	Z	Z10
20	Linear displacement	11	X	X11
21	Linear displacement	11	Y	Y11
22	Linear displacement	11	Z	Z11
23	Linear displacement	12	Y	Y12
24	Linear displacement	12	Z	Z12
25	Linear rate	1	Y	LRY1
26	Linear rate	1	Z	LRZ1
27	Linear rate	2	Z	LRZ2
28	Linear rate	3	X	LRX3
29	Linear rate	3	Y	LRY3
30	Linear rate	3	Z	LRZ3
31	Linear rate	4	Z	LRZ4
32	Linear rate	5	X	LRX5
33	Linear rate	5	Y	LRY5
34	Linear rate	5	Z	LRZ5
35	Linear rate	6	Z	LRZ6
36	Linear rate	7	Y	LRY7
37	Linear rate	7	Z	LRZ7
38	Linear rate	8	Z	LRZ8
39	Linear rate	9	Z	LRZ9
40	Linear rate	10	Z	LRZ10
41	Linear rate	11	X	LRX11
42	Linear rate	11	Y	LRY11
43	Linear rate	11	Z	LRZ11
44	Linear rate	12	Y	LRY12
45	Linear rate	12	Z	LRZ12

Table 2 Telescope actuator description

Actuator (force) no.	Nodal location	Direction	Label
1	1	Y	FY1
2	1	Z	FZ1
3	2	Z	FZ2
4	3	X	FX3
5	3	Y	FY3
6	3	Z	FZ3
7	4	Z	FZ4
8	5	X	FX5
9	5	Y	FY5
10	5	Z	FZ5
11	6	Z	FZ6
12	7	Y	FY7
13	7	Z	FZ7
14	8	Z	FZ8
15	9	Z	FZ9
16	10	Z	FZ10
17	11	X	FX11
18	11	Y	FY11
19	11	Z	FZ11
20	12	Y	FY12
21	12	Z	FZ12

Table 3 Telescope specifications

Output	Title	Label	Value
σ_1	Optical line of sight	LOS_x	65.2 s
σ_2	Optical line of sight	LOS_y	65.2 s
σ_3	Defocus	Defocus	0.001 mm

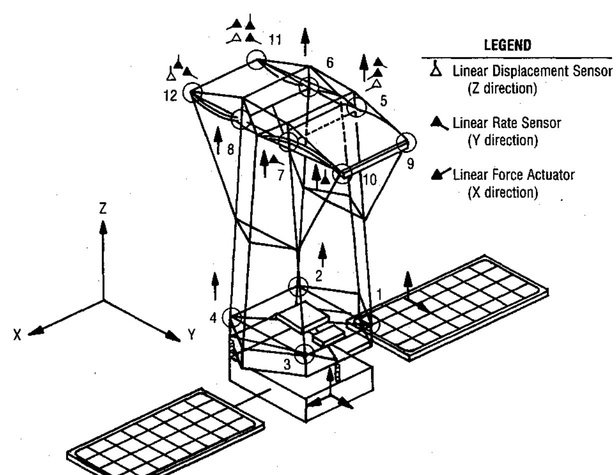

Fig. 2 Telescope sensor and actuator configuration.

bances [i.e., a model S_{tele} (24,3,21,45)]. The development of this model from the NASTRAN data is presented in Ref. 10. The model data is in Appendix C.

The SAS problem for the telescope is as follows.

Telescope SAS Problem

Given: S_{tele} (24,3,21,45) with only 12 actuators and 12 sensors available for designing an LQG regulator to achieve the σ of Table 3.

Required: Specify the closed-loop system that satisfies Eq. (17).

Table 4 shows the iterations of the SAS algorithm when applied to the space telescope. Three observations are worth noting. First, in iteration 1 of the algorithm, the measurements of the outputs were deleted. This might appear disturbing, but two things should be remembered: the algorithm guarantees measurability of the system and the goal of the Kalman-Bucy filter is to estimate the state of the system and not necessarily the output. In the telescope example, the noise present on the output measurements made them unattractive to the filter. Second, despite sensor deletion, the average input value decreased from iterations 1-3. This is dramatic empirical proof of Theorem 1 and indicates that the controller is more efficient at holding the system outputs to specification with 19 actuators than it is with 20 or 21. Furthermore, the rise of average actuator power at iteration 4 suggests that the optimal number of actuators for this design lies between 19 and 15. Third, the algorithm converged to a configuration in only 10 iterations. A direct-search algorithm could have taken thousands of iterations even with the aid of gradient calculations.

Figure 2 shows the sensor and actuator configuration chosen by the SAS algorithm for the telescope example.

Some striking features of this data are no force actuators in the x and y directions at the top of the telescope (i.e., nodes 5-12) and no sensors at the base of the telescope (i.e., nodes 1-4). It appears that the algorithm is making use of the telescope's rigidity in the z direction (i.e., LOS direction) and the flexibility (i.e., motion sensitivity) of the telescope's upper panel in designing an efficient regulator. Several other 12-sensor and 12-actuator configurations have been tested and none performed as well as this configuration.[10]

Table 4 Telescope SAS algorithm results

Iteration no.	Identified sensor, V_i^{sen}	Identified actuator, V_i^{act}	Average input value	Number sen/act
1	Y3 (0.008197) Y1 (0.008195) LOS_y(0.000015) LOS_x(0.000002) Defocus (0)	FX11 (−7.980)	7.483	45/21
2	Z5 (0.02955) Z7 (0.02955)	FX5 (−8.796)	7.393	40/20
3	Y12 (0.03848) Y7 (0.03848) Y11 (0.03848) Y5 (0.03484) Z2 (0.03835) Z4 (0.03835) Z1 (0.03570) Z3 (0.03570) Z6 (0.03460) Z8 (0.08460)	FY7 (−4.003) FY12 (−4.003) FY11 (−4.003) FY5 (−4.003)	7.221	38/19
4	Z10 (0.08602) Z9 (0.08602) X3 (0.08277)	FZ11 (−4.8877) FZ12 (−4.8877)	7.789	28/15
5	LRY3 (0.10815) LRY1 (0.10813)	FZ9 (−5.414)	8.155	25/13
6	LRZ7 (0.12273) LRZ5 (0.11553)	—	8.339	23/12
7	LRZ1 (0.16805) Z11 (0.16129) LRZ6 (0.13838) LRZ8 (0.13615)	—	8.359	21/12
8	LRX3 (0.2237) LRZ2 (0.2191) LRZ4 (0.2077) LRZ3 (0.1960)	—	8.416	17/12
9	LRZ9 (0.47256)	—	8.492	13/12
10	—	—	8.535	12/12

Table 5 Telescope performance

Output no.	$\sqrt{E_\infty y_i^2}$	Actuator no.	$\sqrt{E_\infty u_i^2}$ (minimum achievable)
1 (LOS_x)	65.2 s	1 (FY1)	0.0244 N
2 (LOS_y)	65.2 s	2 (FZ1)	0.0303 N
3 (Defocus) S)	0.0002 mm	3 (FZ2)	0.0297 N
		4 (FX3)	0.0324 N
		5 (FY3)	0.0251 N
		6 (FZ3)	0.0265 N
		7 (FZ4)	0.0338 N
		8 (FZ5)	0.0245 N
		9 (FZ6)	0.0242 N
		10 (FZ7)	0.0221 N
		11 (FZ8)	0.0273 N
		12 (FZ10)	0.0437 N

Table 5 shows the output specifications achieved by this regulator and the root-mean-square (rms) power of each actuator.

The rms power, expressed in Newtons (N), gives the controls engineer actuator-sizing information for the controller design. It also provides a measure of the importance of each actuator in the controller. This information is useful in reliability and redundancy considerations for the actuator configuration.

A final note is the value of the defocus output. The value (0.0002 mm) is well below the σ of 0.001 mm. This seems to indicate that the controller is working too hard and less actuator power would be required if the defocus operated at 0.001 mm. However, for this model, the defocus output is linearly dependent upon LOS_x and LOS_y (i.e., the defocus output could have been deleted from the model). The algorithm LQGWTS looks for output dependency and assigns a zero weighting to dependent outputs to delete them from the model.

V. Conclusion

In summary, the SAS algorithm aids the controls engineer in specifying a sensor and actuator configuration for regulation of large-scale, linear, stochastic systems. The algorithm uses an LQG controller, an efficient weight-selection technique based upon successive approximation, and a measure of sensor and actuator effectiveness to specify a final sensor and actuator configuration. This configuration enables the closed-loop system to meet output specifications with minimal input power. Also, the algorithm involves no complex gradient calculations and has proven numerically tractable for large linear models. This tractability is demonstrated by the space telescope example presented in Sec. IV. Finally, the algorithm provides the controls engineer with information on the important design issues of actuator sizing, reliability, redundancy, and optimal number.

Appendix A: LQG Weight Selection

The successive-approximation technique (LQGWTS) adjusts the diagonal Q and R matrices in the LQG controller so that the closed-loop system satisfies variance constraints on inputs, outputs, or both. The technique evolved through Refs. 10, 13, and 14. This appendix presents a summary of the LQGWTS' theory applying to the minimum-power SAS problem.

For the minimum-power problem, each iteration of the SAS algorithm requires LQGWTS to design a closed-loop system meeting output variance specifications, while minimizing actuator power

$$\sum_{i=1}^{m} E_\infty u_i^2$$

LQGWTS does this by first setting R equal to the identity matrix. This allows the LQG controller to consider all actuators equally and permits the term

$$\sum_{i=1}^{m} E_\infty u_i^2$$

to appear directly in the cost function V of Eq. (6), thus insuring its minimization. LQGWTS then adjusts Q using the following iterative equations:

$$q_i(1) = 1/\sigma_i^2, \qquad i = 1,\ldots,k$$

$$q_i(j+1) = \left[E_\infty y_i^2(j)/\sigma_i^2\right]^{\text{pwr}(j)} q_i(j), \qquad j = 1,2,\ldots \quad \text{(A1)}$$

$$\text{pwr}(1) = 1, \qquad \text{pwr}(j) = j-1, \qquad \forall j > 1$$

where q_i is the ith diagonal entry of Q, and j is the jth iteration of LQGWTS.

The update expression in Eq. (A1) always adjusts q_i in the right direction. The exponent pwr(j) is used to speed up convergence (i.e., increase step size). To prevent overshoot, LQGWTS incorporates a descent function defined as

$$\text{descent}(j+1) = \max\left[E_\infty y_i^2(j+1)/\sigma_i^2 - 1),\ 0\right] \quad \text{(A2)}$$

If descent $(j+1) >$ descent(j), LQGWTS returns to the jth iteration, resets the pwr function to 1 (i.e., the smallest step size), and continues.

As mentioned in Sec. IV, LQGWTS checks for dependent outputs and removes them from the model. The check LQGWTS applies is

$$\text{If } q_i < \epsilon/\sigma_i, \qquad \text{then } q_i \equiv 0 \ (\epsilon \ll 1) \quad \text{(A3)}$$

where setting $q_i = 0$ removes the ith output from the model.

When used for the telescope SAS example, LQGWTS converged in 9 or fewer iterations for each iteration of the SAS algorithm. The major advantage of LQGWTS is its lack of cumbersome gradient calculations. Additionally, it has demonstrated "good" convergence properties on substantial problems in Refs. 10 and 12–14.

Appendix B: Actuator and Sensor Effectiveness Values

The effectiveness values in Eqs. (15) and (16) are derived from closed-loop input cost analysis (CICA) and closed-loop output cost analysis (COCA). Both CICA and COCA are extensions of component cost analysis (CCA) developed by Skelton and co-workers in the late 1970's and early 1980's. CICA and COCA, along with the sensor and actuator effectiveness values, are discussed in detail in Refs. 10–12. This appendix briefly presents the important details applying to the telescope SAS problem.

The fundamental concept behind CICA and COCA is to identify the contribution each input and output of Eq. (8) is making to the cost functional V of Eqs. (6). With these contributions identified, they are combined to determine the effectiveness of each input and output to the control effort.

Using the closed-loop model [Eqs. (8)], the following input and output costs are defined:

$$V_i^u \equiv \tfrac{1}{2} E_\infty\left\{(\partial \bar{y}^T \bar{Q} \bar{y}/\partial u_i) u_i\right\} \quad \text{(B1)}$$

which is the contribution ith control is making to V.

$$V_i^{w_a} \equiv \tfrac{1}{2} E_\infty\left\{(\delta \bar{y}^T \bar{Q} \bar{y}/\delta w_{a_i}) w_{a_i}\right\} \quad \text{(B2)}$$

which is the contribution ith actuator noise is making to V.

$$V_i^v \equiv \tfrac{1}{2} E_\infty\left\{(\partial \bar{y}^T \bar{Q} \bar{y}/\partial v_i) v_i\right\} \quad \text{(B3)}$$

which is the contribution ith sensor noise is making to V.

Applying these definitions to the closed-loop model [Eqs. (8)] yields the following formulas:

$$V_i^u \equiv \left[G\hat{X}G^T R\right]_{ii}, \qquad i = 1,\ldots,m \quad \text{(B4)}$$

where the subscript ii means ith diagonal element of matrix.

$$V_i^{w_a} \equiv \left[B^T(K+L)BW^a\right]_{ii}, \qquad i = 1,\ldots,m \quad \text{(B5)}$$

$$V_i^v \equiv \left[F^T LFV\right]_{ii}, \qquad i = 1,\ldots,l \quad \text{(B6)}$$

where the matrix L satisfies the following steady-state Lyapunov equation:

$$L(A-FM) + (A-FM)^T L + G^T RG = 0 \quad \text{(B7)}$$

Equations (B4–B6) and some useful properties are derived in Refs. 10 and 11. These equations are the basis for V_i^{act} and V_i^{sen} defined in Eqs. (15) and (16).

As noted previously, V_i^u represents the contribution that u_i is making to V. Since the function of LQG theory is to use u_i to minimize V (for a given Q and R), a large V_i^u means that u_i is important to the minimization effort. Alternatively, the contribution that the ith actuator noise source makes to $V\,(V_i^w a)$ is clearly an undesirable contribution. These facts coupled with additional rationale discussed in Refs. 10–13 produce

$$V_i^{\text{act}} \equiv V_i^u - V_i^{w_a} \quad \text{(B8)}$$

Substituting Eqs. (B4) and (B5) into Eq. (B8) gives Eq. (16). A modification to Eq. (B8) accounting for constrained-actuator power is presented in Ref. 10. A modification is also developed in Ref. 19 to account for noise correlations.

As previously noted, V_i^v is the contribution that the ith sensor noise source makes to V. Therefore, those sensors with larger values for V_i^v are contributing more noise to V than those with a smaller V_i^v and, at first glance, appear to be candidates for deletion. However, the sensor measurements for systems $S(n,k,m,l)$ under LQG regulation are passed through a Kalman-Bucy filter. One of the purposes of this filter is to de-emphasize or throw out measurements that have more noise than estimation information. Therefore, any noise source making a "large" contribution to V comes from a sensor that is making an even larger contribution to the estimation information necessary to minimize V. Consequently, the following effectiveness value is defined:

$$V_i^{\text{sen}} \equiv V_i^v \quad \text{(B9)}$$

Substituting Eq. (B6) and the definition for F in Eq. (8) into Eq. (B9) yields Eq. (15). Additionally, Ref. 19 presents a modification to Eq. (B9) accounting for noise correlations.

Appendix C: Telescope Model Data

This appendix presents the contents of the A, B, C, D, M, W, and V matrices for the telescope model $S(24,3,21,45)$.

$$A = \begin{bmatrix} \Omega & S & O_{10} \\ O_4 & \Omega_s & O_{10} \\ O_4 & O & \Phi \end{bmatrix}, \quad B = \begin{bmatrix} O_8 \\ BE \\ O_6 \\ BR \end{bmatrix}, \quad D = \begin{bmatrix} O_8 & O_{18} \\ BE & I_2 \\ O_6 & O_2 \\ BR & O_2 \end{bmatrix} \quad \text{(C1)}$$

$$C = \begin{bmatrix} CE & O^{12} & CR & O^2 \end{bmatrix} \quad \text{(C1)}$$

$$M = \begin{bmatrix} CE & O^{12} & CR & O^2 \\ ME & O^{12} & MR & O^2 \\ O^8 & ME & O^6 & MR \end{bmatrix} \quad \text{(C2)}$$

$$W = \begin{bmatrix} W^a & O_{21} \\ O_2 & W^o \end{bmatrix}, \qquad V = \begin{bmatrix} V_1 & O_2 & O_2 \\ O_{22} & V_2 & O_{22} \\ O_{21} & O_{21} & V_3 \end{bmatrix} \tag{C3}$$

Table C1 The S matrix (8×2)

Row	Column 1	Column 2
1	−1.5105E−03	6.1789E−03
2	8.0569E−04	−9.4151E−05
3	−5.1719E−03	−7.4586E−04
4	1.0263E−03	1.4033E−03
5	7.8788E−03	−5.0280E−03
6	−3.0956E−03	−4.2834E−03
7	−3.5394E−03	−5.3071E−04
8	1.3823E−04	2.2141E−02

The terms in the preceding matrices are defined below:

$$\Omega \equiv \begin{bmatrix} O_8 & I_8 \\ -w^2 & -2\sigma \end{bmatrix}$$

O_8 ≡ null matrix with 8 rows
I_8 ≡ 8×8 identity matrix
w^2 ≡ 8×8 diagonal matrix of squared modal frequencies
2σ ≡ 8×8 diagonal modal damping matrix
w^2 = diag[0.835, 2.736, 3.971, 4.378, 7.746, 13.175, 13.339, 59.112] (rad^2/s^2)
2σ = diag[0.00183, 0.00331, 0.00399, 0.00418, 0.00557, 0.00726, 0.00730, 0.0154] (rad/s)
S ≡ 8×2 coupling matrix (defined in Table C1)

$$\Omega_s = \begin{bmatrix} O_2 & I_2 \\ -w_s^2 & -2\sigma_s \end{bmatrix}$$

Table C2 The BE matrix (8×21)

Row	1	2	3	4	5	6	7
1	6.740E−05	−1.520E−03	−1.507E−03	1.946E−03	−6.628E−05	1.521E−03	1.507E−03
2	−4.615E−03	9.353E−04	7.917E−04	−7.844E−03	4.612E−03	−9.354E−04	−7.911E−04
3	−2.582E−04	−5.140E−03	−5.175E−03	2.359E−06	−2.581E−04	−5.140E−03	−5.175E−03
4	−4.927E−03	−7.887E−04	1.479E−03	1.084E−06	−4.930E−03	−7.889E−04	1.480E−03
5	2.786E−04	7.798E−03	7.885E−03	−7.174E−06	2.784E−04	7.798E−03	7.885E−03
6	1.557E−02	2.626E−03	−4.516E−03	−6.149E−05	1.558E−02	2.607E−03	−4.546E−03
7	−3.792E−04	−3.451E−03	−3.544E−03	1.705E−02	4.814E−04	3.468E−03	3.514E−03
8	−6.065E−05	8.113E−05	1.475E−04	4.850E−04	6.065E−05	−8.125E−05	−1.471E−04

Row	8	9	10	11	12	13	14
1	−6.035E−03	8.661E−05	−1.517E−03	−1.510E−03	−8.696E−05	1.517E−03	1.510E−03
2	−1.575E−03	−4.944E−03	9.175E−04	8.049E−04	4.942E−03	−9.180E−04	−8.050E−04
3	−3.486E−08	−3.288E−04	−5.152E−03	−5.172E−03	−3.290E−04	−5.152E−03	−5.172E−03
4	−4.465E−09	−3.893E−04	−3.367E−04	1.026E−03	−3.896E−04	−3.366E−04	1.027E−03
5	1.040E−07	4.498E−04	7.831E−03	7.879E−03	4.502E−04	7.831E−03	7.879E−03
6	2.331E−06	1.257E−03	1.212E−03	−3.095E−03	1.250E−03	1.190E−03	−3.124E−03
7	−4.789E−04	−5.916E−04	−3.473E−03	−3.540E−03	5.986E−04	3.481E−03	3.519E−03
8	−3.086E−04	6.402E−05	9.512E−05	1.417E−04	−6.462E−05	−9.552E−05	−1.408E−04

Row	15	16	17	18	19	20	21
1	−1.522E−03	1.522E−03	−6.313E−03	8.542E−05	−1.504E−03	−8.536E−05	1.503E−03
2	1.042E−03	−1.043E−03	1.452E−02	−4.945E−03	6.931E−04	4.945E−03	−6.904E−04
3	−5.132E−03	−5.132E−03	2.594E−07	−3.290E−04	−5.195E−03	−3.290E−04	−5.195E−03
4	−1.928E−03	−1.929E−03	−3.986E−07	−3.892E−04	2.617E−03	−3.894E−04	2.618E−03
5	7.786E−03	7.786E−03	−5.702E−07	4.501E−04	7.933E−03	4.504E−04	7.933E−03
6	6.250E−03	6.236E−03	−1.038E−05	1.256E−03	−8.125E−03	1.248E−03	−8.162E−03
7	−3.405E−03	3.446E−03	1.473E−03	−5.928E−04	−3.611E−03	6.008E−04	3.558E−03
8	6.075E−05	−6.123E−05	−5.088E−04	5.993E−05	1.824E−04	−5.937E−05	−1.824E−04

Table C3 The BR matrix (2×21)

Row	1	2	3	4	5	6	7
1	4.931E−06	3.908E−06	−4.849E−06	0	4.931E−06	3.908E−06	−4.849E−06
2	−4.576E−07	3.273E−06	3.273E−06	−5.119E−06	4.576E−07	−3.273E−06	−3.273E−06

Row	8	9	10	11	12	13	14
1	0	−1.258E−05	2.156E−06	−3.097E−06	−1.258E−05	2.156E−06	−3.097E−06
2	1.148E−07	−4.576E−07	3.273E−06	3.273E−06	4.576E−07	−3.273E−06	−3.273E−06

Row	15	16	17	18	19	20	21
1	8.286E−06	8.286E−06	0	−1.258E−05	−9.227E−06	−1.258E−05	−9.227E−06
2	3.273E−06	−3.273E−06	1.296E−05	−4.576E−07	3.273E−06	4.576E−07	−3.273E−06

Table C4 The CE matrix (3×8)

Row	1	2	3	4	5	6	7	8
1	−2.532E−07	−3.478E−07	1.295E−06	2.283E−04	6.032E−06	−7.338E−04	−2.296E−06	1.021E−06
2	3.253E−04	2.145E−04	3.471E−07	−4.422E−07	1.066E−06	6.735E−06	−8.727E−04	2.360E−04
3	−5.025E−08	1.100E−06	5.215E−06	2.761E−06	1.552E−05	−1.016E−05	4.061E−07	4.992E−08

Table C5 The *CR* matrix (3×2)

Row	Column 1	2
1	1	0
2	0	1
3	0	0

w_s^2 ≡ 2×2 diagonal matrix of squared disturbance frequencies

$2\sigma_s$ ≡ 2×2 diagonal disturbance damping matrix

w_s^2 = diag[3947.8, 986.96] (rad²/s²)

$2\sigma_s$ = diag[0.1257, 0.0628] (rad/s)

$$\Phi \equiv \begin{bmatrix} O_2 & I_2 \\ O_2 & O_2 \end{bmatrix}$$

Φ ≡ telescope rigid-body rotational modes (Θ_x, Θ_y)

BE ≡ 8×21 matrix transpose of modal eigenvectors (defined in Table C2)

BR ≡ 2×21 matrix transpose of rigid-body eigenvectors (defined in Table C3)

CE ≡ 3×8 matrix of linear combinations of modal eigenvectors required by system output (defined in Table C4)

O^{12} ≡ null matrix with 12 columns

CR ≡ 3×2 matrix of rigid-body contribution to system outputs (defined in Table C5)

ME ≡ 21×8 matrix of linear combinations of modal eigenvectors required by system measurements (defined in Table C6)

MR ≡ 21×2 matrix of rigid-body contribution to system measurements (defined in Table C7)

$W^a \equiv (0.1)I_{21}$ (N²), $W^o \equiv (3.95)I_2$ (N²)

$V_1 \equiv (0.0001)I_2$ (rad²), $V_2 \equiv (0.000001)I_{22}$ (m²)

$V_3 \equiv (1\times10^{-7})I_{21}$ (m²/s²)

Acknowledgment

This research was sponsored by the U.S. Air Force Academy Department of Astronautics.

Table C7 The *MR* matrix (21×2)

Row	Column 1	2
1	5.632E+00	−4.545E−07
2	4.463E+00	4.000E+00
3	−5.537E+00	4.000E+00
4	0	−5.632E+00
5	5.632E+00	4.545E−07
6	4.463E+00	−4.000E+00
7	−5.537E+00	−4.000E+00
8	0	1.437E+01
9	−1.437E+01	−4.545E−07
10	2.463E+00	4.000E+00
11	−3.537E+00	4.000E+00
12	−1.437E+01	4.545E−07
13	2.463E+00	−4.000E+00
14	−3.537E+00	−4.000E+00
15	9.463E+00	4.000E+00
16	9.463E+00	−4.000E+00
17	0	1.437E+01
18	−1.437E+01	−4.545E−07
19	−1.054E+01	4.000E+00
20	−1.437E+01	4.545E−07
21	−1.054E+01	−4.000E+00

References

[1]Likins, P. W., "Dynamics and Control of Flexible Space Vehicles," Jet Propulsion Lab., TR32-1329, Rev. 1, Jan. 1970.

[2]Balas, M. J., "Trend in Large Space Structure Control Theory: Fondest Hopes, Wildest Dreams," *IEEE Transactions on Automatic Control,* Vol. AC-27, June 1982, pp. 522–535.

[3]Kissel, G. J. and Lin, J. G., "Spillover Prevention Via Proper Synthesis/Placement of Actuators and Sensors," American Control Conference, Arlington, VA, June 1982.

[4]Wu, Y. W., Rice, R. B., and Juang, J. N., "Sensor and Actuator Placement for Large Flexible Space Structures," *Proceedings of the Joint Automatic Control Conference,* Denver, CO, June 1979.

[5]Johnson, T. L., "Principles of Sensor and Actuator Location in Distributed Systems," *Proceedings of NCKU/AAS International Symposium on Engineering Sciences and Mechanics,* Tainan, Taiwan, Dec. 1981.

[6]Gupta, N. A. and Hall, W. E., Jr., "Design and Evaluation of Sensor Systems for State and Parameter Estimation," *Journal of Guidance and Control,* Vol. 1, Nov.–Dec. 1978, pp. 397–403.

[7]Kwakernaak, N. and Sivan, R., *Linear Optimal Control Systems,* Wiley-Interscience, New York, 1972.

[8]Bryson, A. E., Jr. and Ho, Y. C., *Applied Optimal Control,* Ginn and Co., Waltham, MA, 1969.

[9]Athans, M. and Falb, P. L., *Optimal Control,* McGraw-Hill, New York, 1966.

[10]DeLorenzo, M. L., "Selection of Noisy Sensors and Actuators for Regulation of Linear Systems," Ph.D. Thesis, School of Aeronautics and Astronautics, Purdue Univ., West Lafayette, IN, May 1983.

[11]Skelton, R. E. and DeLorenzo, M. L., "Selection of Noisy Actuators and Sensors in Linear Stochastic Systems," *Journal on Large*

Table C6 The *ME* matrix (21×8)

Row	Column 1	2	3	4	5	6	7	8
1	6.740E−05	−4.615E−03	−2.582E−04	−4.927E−03	2.786E−04	1.557E−02	−3.792E−04	−6.065E−05
2	−1.520E−03	9.353E−04	−5.140E−03	−7.887E−04	7.798E−03	2.626E−03	−3.451E−03	8.113E−05
3	−1.507E−03	7.917E−04	−5.175E−03	1.479E−03	7.885E−03	−4.516E−03	−3.544E−03	1.475E−04
4	1.946E−03	−7.844E−03	2.359E−06	1.083E−06	−7.174E−06	−6.149E−05	1.705E−02	4.850E−04
5	−6.628E−05	4.612E−03	−2.581E−04	−4.930E−03	2.784E−04	1.558E−02	4.814E−04	6.065E−05
6	1.521E−03	−9.354E−04	−5.140E−03	−7.889E−04	7.798E−03	2.607E−03	3.468E−03	−8.125E−05
7	1.507E−03	−7.911E−04	−5.175E−03	1.480E−03	7.885E−03	−4.546E−03	3.515E−03	−1.471E−04
8	−6.035E−03	−1.575E−03	−3.486E−08	−4.465E−09	1.040E−07	2.331E−06	−4.789E−04	−3.086E−04
9	8.661E−05	−4.944E−03	−3.288E−04	−3.893E−04	4.498E−04	1.257E−03	−5.916E−04	6.402E−05
10	−1.517E−03	9.175E−04	−5.152E−03	−3.367E−04	7.831E−03	1.212E−03	−3.473E−03	9.512E−05
11	−1.510E−03	8.049E−04	−5.172E−03	1.026E−03	7.879E−03	−3.095E−03	−3.540E−03	1.417E−04
12	−8.696E−05	4.942E−03	−3.290E−04	−3.896E−04	4.502E−04	1.250E−03	5.986E−04	−6.462E−05
13	1.517E−03	−9.180E−04	−5.152E−03	−3.366E−04	7.831E−03	1.190E−03	3.481E−03	−9.552E−05
14	1.510E−03	−8.050E−04	−5.172E−03	1.027E−03	7.879E−03	−3.124E−03	3.519E−03	−1.408E−04
15	−1.522E−03	1.042E−03	−5.132E−03	−1.928E−03	7.786E−03	6.250E−03	−3.405E−03	6.075E−05
16	1.522E−03	−1.043E−03	−5.132E−03	−1.929E−03	7.786E−03	6.236E−03	3.446E−03	−6.123E−05
17	−6.313E−03	1.452E−02	2.594E−07	−3.986E−07	−5.702E−07	−1.037E−05	1.473E−03	−5.088E−04
18	8.542E−05	−4.945E−03	−3.290E−04	−3.892E−04	4.501E−04	1.256E−03	−5.928E−04	5.993E−05
19	−1.504E−03	6.931E−04	−5.195E−03	2.617E−03	7.933E−03	−8.125E−03	−3.611E−03	1.824E−04
20	−8.536E−05	4.945E−03	−3.290E−04	−3.894E−04	4.504E−04	1.248E−03	6.008E−04	−5.937E−05
21	1.503E−03	−6.904E−04	−5.195E−03	2.618E−03	7.933E−03	−8.162E−03	3.558E−03	−1.824E−04

Scale Systems, Theory and Applications, Vol. 4, April 1983, pp. 109–136.

[12]Skelton, R. E. and DeLorenzo, M. L., "Space Structure Control Design by Variance Assignment," *Journal of Guidance, Control, and Dynamics,* Vol. 8, July–Aug. 1985, pp. 454–462.

[13]DeLorenzo, M. L. and Skelton, R. E., "Weight Selection for Variance-Constrained LQG Regulators with Application to the Hoop-Column Antenna," *Fourth VPI & SU/AIAA Symposium on Dynamics and Control of Large Structures,* Blacksburg, VA, June 1983.

[14]Skelton, R. E. and DeLorenzo, M. L., "On Selection of Weighting Matrices in the LQG Problem," *20th Annual Allerton Conference on Circuit and System Theory,* Allerton, IL, Oct. 1982, pp. 803–812.

[15]Chiu, D., *Optimal Sensor/Actuator Selection, Number, and Placement for Linear Stochastic Systems,* Purdue Univ., West Lafayette, IN, TR, Contract 955369, May 1981.

[16]Juang, J. N. and Rodriguez, G., "Formulations and Applications of Large Structure Actuator and Sensor Placements," *Second VPI & SU/AIAA Symposium on Dynamics and Control of Large Flexible Spacecraft,* June 21–23, 1979.

[17]Ichikawa, A. and Ryan, E. P., "Sensor and Controller Location Problems for Distributed Parameter Systems," *Automatica,* Vol. 15, 1979, pp. 347–352.

[18]Hughes, P. C. and Skelton, R. E., "Stability, Controllability, and Observability of Linear Matrix Second-Order Systems," *Proceedings of the Joint Automatic Control Conference,* Denver, CO, June 1979, pp. 56–62.

[19]Norris, G. A., "Selection of Non-ideal Noisy Sensors and Actuators in the Control of Linear Systems," M.S. Thesis, School of Aeronautics and Astronautics, Purdue Univ., West Lafayette, IN, Dec. 1987.